Inhibition in the propagation of fast electrons in plastic foams by resistive electric fields

D. Batani,[1] A. Antonicci,[1] F. Pisani,[1] T. A. Hall,[2] D. Scott,[2] F. Amiranoff,[3] M. Koenig,[3] L. Gremillet,[3] S. Baton,[3] E. Martinolli,[3] C. Rousseaux,[4] and W. Nazarov[5]

[1]*Dipartimento di Fisica "G. Occhialini" and INFM, Università degli Studi di Milano-Bicocca, Piazza della Scienza 3, 20126 Milano, Italy*

[2]*University of Essex, Wivenhoe Park, Colchester, Essex, CO4 3SQ, United Kingdom*

[3]*LULI, UMR No. 7605 CNRS-CEA-X-Paris VI, Ecole Polytechnique, 91128 Palaiseau, France*

[4]*Commisariat a l'Energie Atomique, 91680 Bruyers-le-Chatel, France*

[5]*Department of Chemistry, University of Dundee, Scotland, United Kingdom*

(Received 21 February 2001; revised manuscript received 30 January 2002; published 24 June 2002)

The propagation of relativistic electrons in foam and solid density targets has been studied by means of K-α spectroscopy. Experimental results point out the role of self-generated electric fields in propagation and the role of heating of matter induced by the passage of fast electrons. A simple analytical formulation has been given and Spitzer conductivity has been shown to be fairly compatible with experimental results.

DOI: 10.1103/PhysRevE.65.066409 PACS number(s): 52.38.−r, 52.50.Jm

The ability to produce short, high-energy laser pulses in TW regime as a consequence of the recent developments in laser technology (chirped pulse amplification [1]), has allowed laser intensities on target bigger than 10^{18} W/cm^2 to be obtained, and has produced a large interest in laser-solid interaction experiments. In this new regime, materials are quickly ionized and electrons get accelerated to velocities close to c, so that the domain of relativistic plasma physics becomes accessible [2]. Phenomena such as relativistic self-focusing, particle acceleration, energetic particle production, plasma high harmonics generation, etc., have been evidenced. Among these, the generation of intense beams of relativistic electrons [3,4] ("fast" or "hot" electrons) is interesting both in itself and for its possible application to the proposed concept of "fast ignition" of thermonuclear targets [5]. In this scheme, a laser bores a hole through the plasma corona so that a second beam interacts with the dense part of the target producing fast electrons. They must then propagate to the compressed core and heat it to ignition conditions. The study of fast electron penetration is therefore essential to such a scheme.

As explained in many theoretical and experimental papers, electric effects may cause a reduction of the range of fast electrons as compared to what can be predicted taking into account collisional effects only (so called "electric inhibition"). The electric effects arise from the electric field E generated by charge separation and by inductive effects, as the fast electrons propagate into the target. These electrons carry a current density $J_{\rm hot}$ of magnitude that can be as large as 10^{12} A/cm^2 depending on the specific conditions of laser-target interaction. The magnitude of the electric field E depends instead on the conductivity σ of the target material, $E \approx J_{\rm hot}/\sigma$, because a return current balancing the current of fast electron into the target must be set up to maintain quasineutrality and consequently to allow fast electron propagation.

A significant inhibition can thus be expected, and was evidenced, first of all in targets with low electrical conductivity [6–9]. An even larger inhibition is, however, expected in low-density materials (foams) since a low density means fewer background electrons available to supply the return current.

Let us notice that the problem of the electric inhibition of fast electron propagation is not restricted to solid or near-solid density targets but is also important in a true fast ignitor context, that is, for the propagation of fast electrons inside a hot thermonuclearlike plasma. Indeed for efficient penetration we must have $J_{\rm hot} \approx J_{\rm return}$ where $J_{\rm hot} = (n_{\rm hot} ec)$, and $J_{\rm return} = (n_e e v_e)$, and where $n_{\rm hot}$, n_e, and v_e are, respectively, the density of fast electron in the beam, and the density and mean velocity of free background electrons. Hence, because the return current cannot be faster than c, the current balance implies $n_{\rm hot} \ll n_e$. The violation of this condition in all cases in which the plasma density is not large enough will break down charge neutrality and will result in a strong electric inhibition and/or in a drastic reduction in the number of produced fast electrons (and the energy they carry). This is an additional reason why hole boring may be essential in fast ignition: if the interaction (and hence fast electron production) takes place far from the highest density regions of the target, effective electron penetration may be prevented. (In passing we note how this may indeed be a problem for recent proposals of "fast ignition without hole boring" [10].)

From an experimental point of view, an important aspect is that, as resistivity and inhibition increases, at the same time the collisional effects, described, for example, in terms of stopping power [11], are in first approximation only sensitive to the total areal density of the material crossed by the fast electrons (that is $m = \rho d$, where ρ is the target density and d its thickness). This means that the collisional penetration range of fast electrons, $l_{\rm col}$ (measured in length units) scales as $l_{\rm col} \approx \rho l_0 / \rho_0$, where ρ_0, ρ, and l_0 are, respectively, the standard density of the material, the density of the material in foam state and the collisional penetration range in the material at standard density.

As a result of the different dependence of the two effects (electric and collisional), electric fields soon become the dominant factor in limiting fast electron propagation in foams when the density is decreased. Hence the collisional

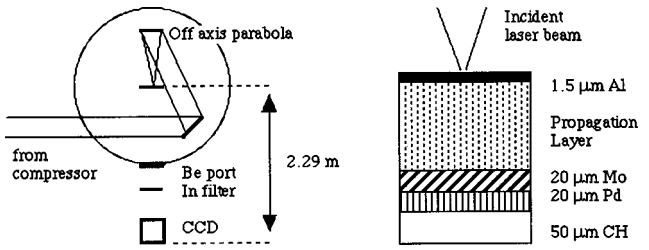

FIG. 1. Experimental setup and scheme of the multilayer target.

range, l_{col}, will become much larger than the electric range, l_{el}, which in first approximation can be determined using the formula by Bell *et al.* [12]

$$l_{\mathrm{el}}(\mu\mathrm{m}) \approx 3\times 10^{-3}\sigma_{\mathrm{foam}}(T_{\mathrm{hot}})^2/\eta I_L, \tag{1}$$

where T_{hot}, η, and I_L are the fast electron temperature, conversion efficiency (from laser pulse energy to fast electron energy), laser intensity on target and conductivity [respectively, in units of keV, 10^{17} W/cm^2, and 10^6 (Ω cm^{-1})]. Indeed foams were already used as early as 1982 by Bond, Hares, and Kilkenny [13] and allowed electric field effects to be evidenced at laser intensities as low as 10^{15} W/cm^2. In this case the "hot" electrons were characterized by $T_{\mathrm{hot}} \approx 12$ keV, i.e., were nonrelativistic.

In the experiment presented in this paper, we used foam targets and studied fast electron propagation in the proposed short-pulse ultrahigh intensity regime that is today available. This is different from the regime investigated by Bond, Hares, and Kilkenny because: (i) relativistic electrons are produced and accelerated into the target, (ii) a much bigger conversion (η) from laser energy to fast electron is obtained. *A priori*, this is likely to produce stronger electric field effects, but also a strong heating of the target material, which will produce dramatic changes in its resistivity (this will somewhat complicate the interpretation of data because the value of conductivity to be used in Bell's formula corresponds to the warm material whose temperature must be calculated consistently with penetration). Moreover, free electrons in the material, contributing to the background conductivity, will also be produced as a result of electric breakdown induced by the very high self-generated electric fields. In particular, heating and breakdown produce a phase change (insulator to conductor) in plastic targets, as shown in Refs. [8,9], allowing for non-negligible fast electron penetration in matter. Hence, it becomes possible to use plastic foams in this kind of experiments whereas Bond, Hares, and Kilkenny used metallic foams only.

Our experimental setup is shown in Fig. 1. We carried out the experiment using the LULI TW laser chain delivering pulses with $\lambda = 534$ nm, duration 350 fs, and a maximum energy ≈ 20 J. The laser beam was focused on the target by means of an off-axis parabola. The focal spot dimension was measured in the far field with an optical charge coupled device (CCD), while a x-ray pinhole camera, placed inside the chamber, measured the size of the produced plasma. Pulse duration was measured with a single shot autocorrelator.

The measured parameters correspond to on-target irradiances of the order of 2×10^{19} W/cm^2. The target was placed in a vacuum chamber, perpendicular to the laser. Variations in laser energy and pulse duration from shot to shot gave a $\pm 20\%$ variance in laser intensity.

We used multilayered targets and K-α emission spectroscopy as the main diagnostic for the propagation of electrons. The laser beam interacts with a first layer of 1.5-μm Al, where the fast electrons are generated and accelerated. This first layer was already used by Bond, Hares, and Kilkenny and in one of our previous papers in which we compared fast electron penetration in conductors and insulators [9]. It is essential in our experiment because it allows the effects of propagation to be separated by those of fast electron production (i.e., the electron source is the same irrespective of the foam density). Also it allows to use the experimental values of T_{hot} and η obtained in Ref. [9] for Al targets with exactly the same setup and laser parameters of the experiments presented here, i.e., $T_{\mathrm{hot}} \approx 500$ keV and $\eta \approx 20\%$.

After this first layer there is the foam ("propagation" layer) in which the fast electrons penetrate before reaching two layers of fluor materials (20 μm of Mo and 20 μm of Pd) where they cause impact ionization followed by K-α x-ray photon emission. Finally, a layer of 50 μm of polyethylene shields the Pd layer and avoids any spurious emission due to the electrons reaching the Pd layer after crossing the target rear side (and pulled back by electric fields). (Notice that the measured penetration depth in plastic is of the order of 180 μm for 500 keV electrons. Hence a 50-μm-thick plastic rear side is sufficient to drastically reduce spurious K-α emission since electrons lose most of their energy before reaching it, and because this must be crossed twice before the electrons come back to the fluor layer.)

To detect the K-α x-rays, we used a 1024×256 pixels CCD camera that was placed outside the vacuum chamber at a distance of about 2 m from the target, to ensure a negligible probability of two photons interacting with the same pixel (single hit, or spectroscopic, mode). In this manner the signal registered from each pixel was proportional to the x-ray photon energy and the resulting image of multiple single counts, allowed to reconstruct the histogram of the x-ray spectrum. Also, the CCD camera was shielded with a 125-μm-indium filter in order to reduce the x-ray intensity.

The foam layers were realized with a technique developed at Dundee University [14]. The monomer used in our experiments was trimethylol propane triacrylate, $C_{15}H_{20}O_6$. Starting from a monomer solution containing a photoinitiator, foams were polymerized *in situ* using UV light inside a brass ring of the required thickness that determined the final thickness of the foam. Uniform foams with measured pore sizes <1 μm were, as shown in scanning electron microscope photographs [15].

We have chosen two different foam densities (0.025 and 0.1 g/cm^3) and the corresponding thickness ($d = 0.2$ and 0.05 cm) so to have the same areal density: 0.005 g/cm^3, which is also the areal density chosen for the layer of solid plastic (which has a density $\rho_0 = 0.96$ g/cm^3 and a thickness $d = 50$ μm). This choice is important because, as previously said, the collisional effects are proportional to areal density

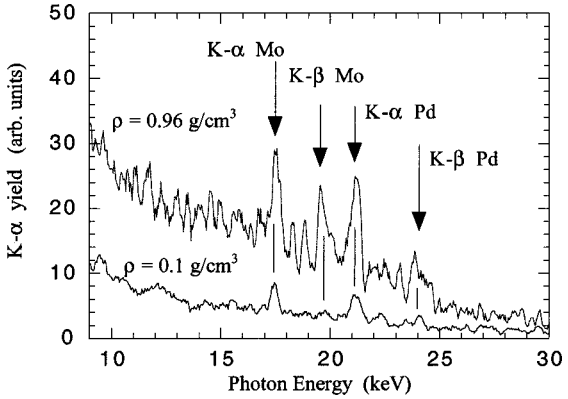

FIG. 2. Typical x-ray spectra collected with the CCD for two densities (respectively $\rho=0.96$ g/cm^3 and $\rho=0.1$ g/cm^3). All other experimental parameters are practically identical. The vertical scale gives the CCD counts. The spectrum is shown before the deconvolution that takes into account the filter effects. The Mo and Pd K-α peaks correspond to photon energies 17.4793 and 21.1771 keV, respectively. The K-β peaks at 19.6083 and 23.8187 keV can also be seen.

of the target. Hence, differences between various target densities will be due to different field effects only.

Figure 2 shows the experimental x-ray spectra obtained in typical shots, showing the Mo and Pd K-α peaks. A data deconvolution technique was applied to take into account charge diffusion between adjacent pixels. Such procedure did reduce data noise but was verified not to change the qualitative trend of experimental data. Figure 3 shows the K-α yield from Mo and Pd plotted against areal density from foams and normal density plastics. The error bars are given by the standard deviation of experimental results. Every point is obtained from the average of six to seven successful laser shots.

As we can see there is an approximate power law scaling with a slope ≈ 0.52 for both Pd and Mo. Since the areal density is the same for all targets ($m \approx 50$ mg/cm^2), the reduction of K-α yield when target density is decreased gives the experimental evidence of inhibition of fast electron penetration, with respect to what can be calculated with collisional models only, and obviously points out to the role of electric inhibition.

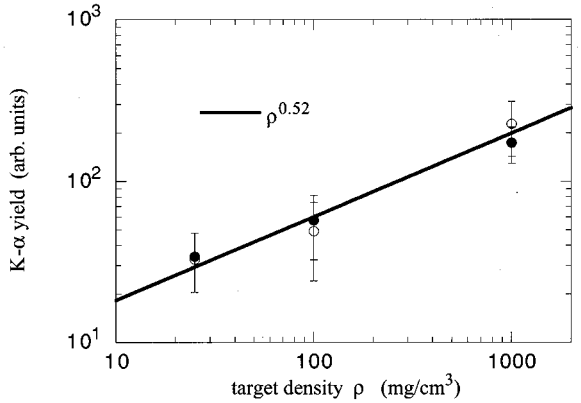

FIG. 3. K-α yield from Mo (black circles) and Pd (white circles) vs target density.

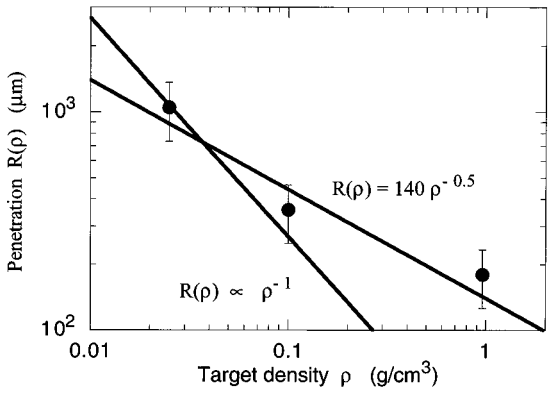

FIG. 4. Calculated penetration range $R(\rho)$ vs target density.

Many recent experimental works have shown that the K-α yield from buried fluor layers decays in approximately an exponential way as a function of target thickness [4,6]. This behavior can be qualitatively understood as follows: monoenergetic electrons have a definite range in matter but because fast electrons produced in laser-plasma interaction are characterized by an energy distribution (approximately exponential) we get an exponential profile for energy deposition. A recent theoretical/numerical work [16] gives a full picture of the phenomenon and shows that, for thick targets (like those usually used in experiments) the profile is indeed exponential. Finally, the work by Pisani *et al.* [9] shows that the K-α yield from 500 keV electrons in plastic, obtained in exactly the same conditions of the present experiment, follows an exponential law, i.e., $K(d)=K_0\exp(-d/R_0)$, where d is the propagation layer thickness, R_0 is the penetration range, and $K(d)$ is the experimental yield. We also estimated that $R_0=180\pm 30$ μm in plastic. Since in our case the constant K_0 is the same for all targets thanks to the presence of the Al layer, we can write the K-α yield from a target with density ρ and thickness d as

$$K(d,\rho)=K_0\exp[-m/\{\rho R(\rho)\}]. \tag{2}$$

Here $R(\rho)$ is the penetration range in a foam target, and the areal density m is the same for all our targets. By comparing the K-α yield from plastic and foam targets, we then obtain

$$\frac{1}{\rho R(\rho)}=\frac{1}{\rho_0 R_0}-\frac{1}{m}\ln\left(\frac{K(\rho)}{K(\rho_0)}\right). \tag{3}$$

Since the penetration range R_0 in normal density plastic is known, this formula allows the penetration $R(\rho)$ in a foam target to be obtained. The values we get from our experimental results are shown in Fig. 4 and scale approximately as $\rho^{-0.5}$. We recall again that instead the collisional penetration is inversely proportional to ρ. [Let us notice that the numerical values of $R(\rho)$ depend on the assumption of exponential deposition, but in order to get the scaling it is only necessary to assume that the profile has the same functional form at all densities.]

In all cases we are in a regime of electric dominated transport. This was shown in Ref. [9] to be true for plastic at normal density (in that case $R_0 \approx 180\ \mu$m while $l_{\rm col} \approx 690\ \mu$m) and will be truer in the case of lower densities. Hence we can neglect the collisional contribution and tentatively identify the experimental values in Fig. 4 with the electric penetration range $l_{\rm el}$ given by Bell.

The experimental scaling then allows some useful considerations. In our case, the changes in $R(\rho)$ are only due to changes in target conductivity σ. The data in Fig. 3 and Fig. 4 shows that $l_{\rm el}$, and hence conductivity, is bigger for lower density foams, but electric inhibition becomes stronger at lower densities (the ratio $l_{\rm col}/l_{\rm el}$ scales as $\approx \rho^{1.5}$). In the following we will develop and discuss a simple heuristic model that reproduces our experimental scaling quite well. In order to calculate σ we must calculate the temperature T (and ionization degree Z^*) in the background material. This will scale as

$$T \approx A E_{\rm hot}/[\pi r^2 \rho R(\rho) Z^* N_A], \tag{4}$$

where A and N_A are the average atomic weight and Avogadro's number, $E_{\rm hot}$ is the energy in the fast electron beam ($=\eta E_L$), and r the actual electron spot radius. In practice we assume the fast electron energy is deposited in a cylindrical volume $[\pi r^2 R(\rho)]$, and the quantity $N_e = [\pi r^2 \rho R(\rho) Z^* N_A/A]$ is the number of free electrons in such a volume. Equation (4) neglects the contribution to the heat capacity of the material from the ionization energy, which can be calculated as $\Delta E \approx N_e I$, where I is the average ionization energy, and is indeed negligible with respect to the energy in the fast electron beam.

The assumption of a cylindrical volume will be discussed later. The value of the electron spot r is usually larger than the laser focal spot radius. Already the shadowgraphy images presented in Ref. [17] showed that fast electron are penetrating in the target from a surface area that is substantially larger than the focal spot.

By using the typical parameters of our experiment, and a value of r of the order of a few times the focal spot radius, we can evaluate temperatures of the order of $\approx$100 eV, in the case of normal density plastic, and quite higher for more tenuous foams. The increase in temperature when ρ is decreased is not only a consequence of Eq. (2) but is already implied by our experimental results on the reduction of K-α yield, reduction of penetration range, when target density is decreased.

The important point is now that at such high temperatures, the conductivity of all materials is expected to follow a Spitzer-like behavior, according to which [18]

$$\sigma(\Omega\ {\rm cm})^{-1} = 97.09 T^{3/2}/(Z^* \ln\Lambda), \tag{5}$$

where T is in eV and $(\ln\Lambda)$ is the Coulomb logarithm. For instance, in the case of Al, the experimental measurements of Milchberg *et al.* [19] (and their analytical interpolation done by Davies *et al.* [20]) show that Spitzer conductivity sets up at temperatures of the order of $T \leqslant 100$ eV. In the case of plastics at normal density, simple models also suggest that Spitzer conductivity becomes appropriate at $T \leqslant 100$ eV [8].

Moreover we can practically expect the ionization to be almost complete (foams being composed of low-Z elements only). Hence the material conductivity becomes independent (explicitly) on the density ρ, and is dependent on temperature T only (which, however, depends on density). By coupling Eqs. (1), (4), and (5), and recalling that we have identified $l_{\rm el}$ and $R(\rho)$, we can derive that

$$l_{\rm el} \propto \sigma_{\rm foam} \approx [97.09 T^{3/2}/(Z^* \ln\Lambda)] \propto [\{\rho R(\rho)\}^{-1}]^{3/2}, \tag{6}$$

which finally gives a scaling $R(\rho) \propto \rho^{-3/5} = \rho^{-0.6}$. This must certainly be considered in very good agreement with our experimental results, seeing all the approximations used in our simple heuristic model. Let us notice that completely different scaling laws are obtained if we assume a semiclassical behavior of resistivity (as done, for instance, in Ref. [8]) or a semispherical propagation of fast electrons (as would be appropriate to a strongly collisional case).

In this regime, we can derive the scaling laws for the other relevant quantities. In particular the conductivity σ scales as $\propto \rho^{-3/5}$, the electric field E scales as $\propto \rho^{3/5}$, and the temperature T scales as $\propto \rho^{-2/5}$. All this follows from Spitzer's and Bell's formulas that imply that the propagation range no longer follows the expected collisional (ρ^{-1}) dependence.

Despite the fairly good agreement between our experimental results and the simple model, one should really be concerned about the fact that the role of magnetic fields and their relation with the background foam density have been neglected in the discussion (apart from the fact that they are assumed to be strong enough to produce a quasicylindrical propagation of the fast electrons). Indeed the main assumption of the model concerns the geometry of the fast electron beam. A quasicylindrical propagation is not unrealistic since the large self-generated magnetic fields can induce beaming. This self-pinching of the beam has been first theoretically predicted [20], and recent experimental results [17] have been interpreted as giving evidence of fast electron collimated propagation.

However, the situation is far more complicated. Even if we do expect large magnetic fields connected to the large fast electron currents, their actual estimate is difficult because it depends on the geometry of the current and on the magnitude of the return current (and hence on background conductivity). Also, the fast electron current exceeds the well-known Alfven limit by many orders of magnitude, implying again the need for a strong return current. Recent theoretical and numerical works have shown that, during propagation, the fast electron current may suffer a strong filamentation, connected either to a Weibel-like instability [21] or to an electrothermal instability [22]. Inside each filament the return current will approximately balance the fast electron current, thereby probably the net filament current will be of the order of the Alfven limit. On the time scale of $\approx$100 fs, these filaments begin to coalesce due to their mutual magnetic interaction. Coalescence of two adjacent filaments will result in a single filament, again carrying a net current of the order of the Alfven limit, with a net energy loss which has been

described as an anomalous collective stopping power [23]. Simulations have also shown [24] that the growth rate of the instability is larger for more tenuous foams, and that the effect of the collective stopping power increases as the density of the fast electron beam becomes larger relatively to the background electron density (i.e., the collective stopping power is larger for more tenuous foams). On the other side, Davies *et al.* [20] predict that the magnetic fields increases when the conductivity is larger (as a consequence of the relation between magnetic and electric fields in this context), and hence more tenuous foams correspond to smaller magnetic fields inside matter (since, as we have shown before, temperature and conductivity here are larger).

Despite their obvious interest, the meaning of such simulations with respect to our experimental results is not obvious. At present, detailed simulations performed with PIC codes do not allow to follow fast electron propagation over the required time scale and target size ($\leqslant 7$ ps and $\leqslant 2$ mm, respectively) and also they are affected by important limitations (collisions are usually neglected, electron densities corresponding to solid materials cannot be simulated, etc.). Electromagnetic hybrid codes can work on the required time and space scales but are also affected by several limits (two-dimensional, description of material resistivity, neglect of electrostatic fields induced by charge separation, etc.). Hence we might speculate that, on long space and time scales, subsequent coalescence of filaments may finally result in a collimated propagation of fast electrons or in the formation of a bunch of no-longer-interacting filaments. Then, it is important to notice that the scaling given by Eq. (4) holds even if instead of propagation in an uniform cylinder, fast electrons will propagate in a bunch of filaments. Of course in this case Eq. (4) will give the temperature averaged over the different filaments. Instead Eq. (4) will not hold whenever the different filaments coalesce in space and/or in time.

In conclusion we can summarize the content of this work in the following points:

(i) we have shown how the use of low-density foams is a suitable experimental technique to maximize the inhibition of fast electron penetration in matter;

(ii) we have shown how the correct calculation of fast electron penetration under electric limited fast electron transport (i.e., $l_{\mathrm{col}} \gg l_{\mathrm{el}}$) requires a consistent calculation of temperature and conductivity of the background material;

(iii) we have implicitly shown how, in the conditions of our experiment, matter is heated to quite high temperatures where it is appropriate to use Spitzer's conductivity;

(iv) we have developed a simple heuristic model and derived a theoretical scaling for the penetration range vs target density (which is valid in the Spitzer limit) and for the other relevant quantities (E, T, σ).

This work was supported by the TMR European Program, Contract No. ERBFMGECT950044 and in part by Grant No. E1127 from Région Île-de-France. The participation of A.A was possible within the Erasmus agreement between Università di Milano-Bicocca and Ecole Polytechnique.

[1] See, for instance, C. N. Danson *et al.*, J. Mod. Opt. **45**, 1653 (1998).

[2] see, for instance, S. V. Bulanov, F. Califano, G. I. Dudnikova, T. Zh. Esirkepov, I. N. Inovenkov, F. F. Kamenets, T. V. Liseikina, M. Lontano, K. Mima, N. M. Naumova, K. Nishihara, F. Pegoraro, H. Ruhl, A. S. Sakharov, Y. Sentoku, V. A. Vshivkov, and V. V. Zhakhovskii, Rev. Plasma Phys. **22**, 1 (2001).

[3] M. Tatarakis *et al.*, Phys. Rev. Lett. **81**, 999 (1998); D. B. Melrose *et al.*, J. Plasma Phys. **62**, 233 (1999); T. Phillips *et al.*, Rev. Sci. Instrum. **70**, 1213 (1999); P. A. Norreys *et al.*, Phys. Plasmas **6**, 2150 (1999); K. W. D. Ledingham *et al.*, Phys. Rev. Lett. **84**, 899 (2000); G. Malka and J. L. Miquel, *ibid.* **77**, 75 (1996); Th. Schlegel *et al.*, Phys. Rev. E **60**, 2209 (1999); M. E. Glinsky, Plasma Phys. Rep. **2**, 2796 (1995); S. Wilks *et al.*, Phys. Rev. Lett. **69**, 1383 (1992); E. T. Gumbrell *et al.*, Phys. Plasmas **5**, 3714 (1998).

[4] F. Beg *et al.*, Phys. Plasmas **4**, 447 (1997).

[5] M. Tabak *et al.*, Phys. Plasmas **1**, 1626 (1994); S. Atzeni, Jpn. J. Appl. Phys., Part 1 **34**, 1980 (1995).

[6] M. Key *et al.*, Phys. Plasmas **5**, 1966 (1998), K. Wharton *et al.*, Phys. Rev. Lett. **81**, 822 (1998).

[7] T. Hall, S. Ellwi, D. Batani, A. Bernardinello, V. Masella, M. Koenig, A. Benuzzi, J. Krishnan, F. Pisani, A. Djaoui, P. Norreys, D. Neely, S. Rose, M. Key, and P. Fews, Phys. Rev. Lett. **81**, 1003 (1998); A. Bernardinello, D. Batani, V. Masella, M. Koenig, A. Benuzzi, J. Krishnan, F. Pisani, A. Djaoui, P. Norreys, D. Neely, S. Rose, T. A. Hall, S. Ellwi, and P. Fews, Laser Part. Beams **17**, 529 (1999).

[8] D. Batani, J. Davies, A. Bernardinello, T. A. Hall, M. Koenig, F. Pisani, A. Djaoui, P. Norreys, D. Neely, and S. Rose, Phys. Rev. E **61**, 5725 (2000).

[9] F. Pisani, A. Antonicci, A. Bernardinello, D. Batani, E. Martinolli, M. Koenig, L. Gremillet, F. Amiranoff, S. Baton, T. Hall, D. Scott, P. Norreys, A. Djaoui, C. Rousseaux, P. Fews, H. Bandulet, and H. Pepin, Phys. Rev. E **62**, R5927 (2000).

[10] S. Hain and P. Mulser, Phys. Rev. Lett. **86**, 1015 (2001).

[11] C. Deutsch *et al.*, Phys. Rev. Lett. **77**, 2483 (1996); V. V. Val'chuk, N. B. Volkov, and A. P. Yalovets, Plasma Phys. Rep. **21**, 159 (1995).

[12] A. R. Bell *et al.*, Plasma Phys. Controlled Fusion **39**, 653 (1997).

[13] D. J. Bond, J. D. Hares, and J. D. Kilkenny, Plasma Phys. **24**, 91 (1982).

[14] J. Falconer *et al.*, J. Vac. Sci. Technol. A **12**, 2798 (1994); J. Falconer *et al.*, *ibid.* **13**, 1941 (1995).

[15] D. Batani, W. Nazarov, T. Hall, Th. Löwer, M. Koenig, B. Faral, A. Benuzzi-Mounaix, and N. Grandjouan, Phys. Rev. E **62**, 8573 (2000).

[16] J. Davies, Phys. Rev. E **65**, 026407 (2002).

[17] L. Gremillet, F. Amiranoff, S. Baton, J. C. Gauthier, M. Koenig, E. Martinolli, F. Pisani, G. Bonnaud, C. Lebourg, C. Rousseaux, C. Toupin, A. Antonicci, D. Batani, A. Bernardinello, T. Hall, D. Scott, P. Norreys, H. Bandulet, and H.

Pepin, Phys. Rev. Lett. **83**, 5015 (1999); M. Borghesi *et al.*, *ibid.* **83**, 4309 (1999).
[18] L. Spitzer, *The Physics of Fully Ionised Gases* (Wiley-Interscience, New York, 1962).
[19] H. M. Milchberg *et al.*, Phys. Rev. Lett. **61**, 2364 (1988).
[20] J. Davies *et al.*, Phys. Rev. E **56**, 7193 (1997).
[21] F. Califano, F. Pegoraro, and S. Bulanov, Phys. Rev. E **57**, 7048 (1998); **56**, 963 (1997); Y. Sentoku, K. Mima, S. Kojima, and H. Ruhl, Phys. Plasmas **7**, 689 (2000).
[22] M. Haines, Phys. Rev. Lett. **47**, 917 (1981).
[23] M. Honda, Phys. Plasmas **7**, 1606 (2000); M. Honda and J. Meyer-ter-Vehn, *ibid.* **7**, 1302 (2000); L. Gremillet, Ph.D. thesis, Ecole Polytechnique, Palaiseau, France, 2001.
[24] M. H. Key, J. Hill, B. Lasinski, B. Langdon, P. Parks, M. Rosenbluth, C. Andersen, T. Cowan, R. Freeman, S. Hatchett, J. Koch, A. MacKinnon, N. Fisch, R. Snavely, and R. Stephens, in *The 5th Workshop on Fast Ignition of Fusion Targets* (Madeira, Portugal, 2001).